

## Supplementary Material

### **High-efficiency reactor and its tandem module with Au-Co-CoO<sub>x</sub>-coated glass beads for continuous-flow reduction of dyeing wastewater**

Li Sun,<sup>\*a</sup> Mengying Sun,<sup>a</sup> Yuan Zhi,<sup>b</sup> Hua Zhang,<sup>a</sup> Yuejin Shan,<sup>c</sup> Binlin Dou,<sup>a</sup> Jian Chen<sup>a</sup> and Lixin Zhang<sup>a</sup>

<sup>a</sup> Shanghai Key Laboratory of Multiphase Flow and Heat Transfer in Power Engineering, School of Energy and Power Engineering, University of Shanghai for Science and Technology, Jun Gong Road 516, Shanghai 200093, China

<sup>b</sup> R&D Department, Shanghai Minrula Biotechnology Co.,Ltd, Building 15, Haji Sixth Road 218, Shanghai 201306, China

<sup>c</sup> Department of Material and Environmental Chemistry, Research Division of Functional Materials Design, Utsunomiya University, Yoto 7-1-2, Utsunomiya 321-8585, Japan

\* Corresponding author: E-mail: marybrother@yeah.net; Tel: +86 21 55272740; Fax: +86 21 55272376

## **Text S1**

### **The C-F reduction of 4-NP in real water samples**

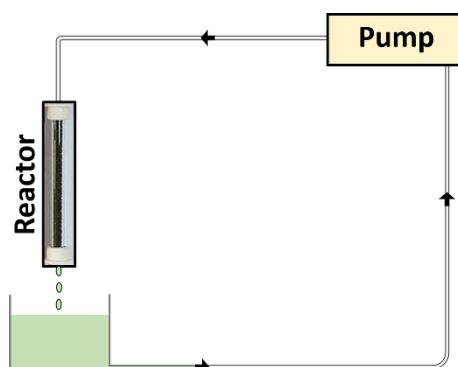
Three water samples are individually taken from local tap water (Laboratory, Shanghai, China), West Lake water (Hangzhou, China) and Huangpu River water (Shanghai, China). Prior to use, solid impurities in water samples are removed by an aspirator filter pump.

The continuous-flow (C-F) reduction of 4-NP is described as follows. Typically, 0.1g of 4-NP was dissolved into 145 mL of water sample to obtain a 4-NP solution. Next, the above 4-NP solution and the NaBH<sub>4</sub> solution were simultaneously injected by a micro-syringe pump into a home-made micro-mixer to form a homogeneous reaction solution. The injection rates of 4-NP and NaBH<sub>4</sub> solutions were same and set at 380~500 mL/h. Afterwards, the reaction solution was further injected into the tandem module. To analyze the catalytic capacity of the tandem module, the C-F reduction of 4-NP was monitored by an UV-Vis spectrophotometer.

## **Text S2**

### **The build of the cycle model and its application**

The cycle model is built, shown in Scheme S1. The reduction of 4-NP to 4-AP is performed in a tubular packed reactor using a peristaltic pump as the driving force. The initial concentrations of 4-NP and NaBH<sub>4</sub> are set at 5 and 12 mM, respectively. The flow rate of the reaction mixture (4-NP and NaBH<sub>4</sub>) is fixed at 760 mL/h. The conversion efficiency of 4-NP to 4-AP under xenon lamp irradiation is determined by a UV-Vis spectrophotometer.



**Scheme S1** The cycle module for the reduction of 4-NP to 4-AP.

**Table S1**

pH values of different water samples

Samples	Deionized Water	West Lake	Huangpu River	Tap Water
pH	7.0	6.78	7.45	7.23

**Table S2**

Effects of the calcination temperature and the Au loading on the performance of the packing material, reflected by the removal rate of 4-NP.

Removal rate of 4-NP ( $\mu\text{mol/h}$ ) Calcination temperature ( $^{\circ}\text{C}$ )	200	300	400	500
Au loading (wt%) *				
0	10	11	10	10
0.25	30	60	59	58
0.45	75	100	98	97
0.75	84	101	100	98

\*The Au loading in the packing material is determined by the EDS analysis.

**Table S3**

The content of Au in packing materials determined by ICP

Packing Materials	Au (wt%)		Loss ratio of Au
	Fresh	Used*	
Au-Co-CoO <sub>x</sub> -coated glass beads	0.452	0.451	0.22%

\*The packing materials is continuously used for 24 h

**Table S4**

The content of Au in packing materials determined by ICP

Packing Materials	Au (wt%)		Loss ratio of Au
	Fresh	Used*	
Au-Co-CoO <sub>x</sub> -coated glass beads	0.451	0.451	0

\* The reused packing material after six months.

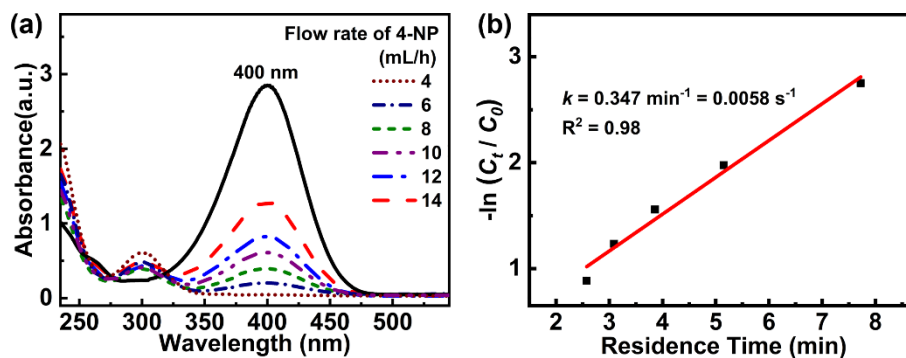


**Fig. S1** (a) UV-Vis spectra for the C-F degradation of 4-NP in the reactor using Au-Co-CoO<sub>x</sub>-coated glass bead as packing material in dark (Solid line represents UV-Vis spectrum of 4-nitrophenolate anions generated by the mixing of NaBH<sub>4</sub> and 4-NP). (b) Plot of  $-\ln(C_t/C_0)$  versus the residence time.

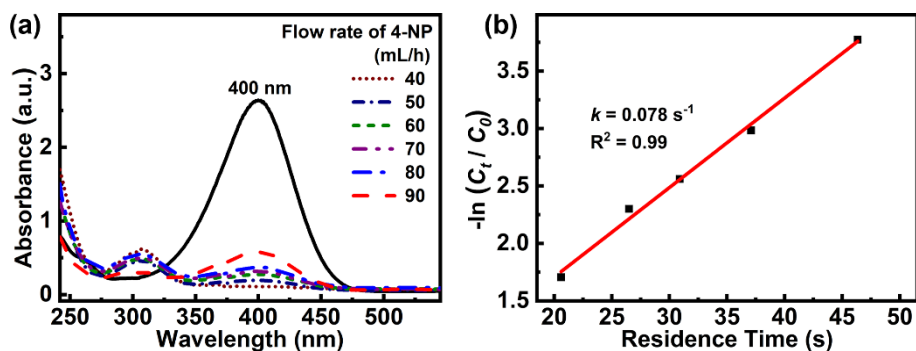


**Fig. S2** (a) UV-Vis spectra for the C-F reduction of 4-NP with a relatively low concentration (0.3 mM) in the reactor using Au-Co-CoO<sub>x</sub>-coated glass bead as packing material (Solid line represents UV-Vis spectrum of 4-nitrophenolate anions generated by the mixing of NaBH<sub>4</sub> and 4-NP). (b) Plot of  $-\ln(C_t/C_0)$  versus the residence time.

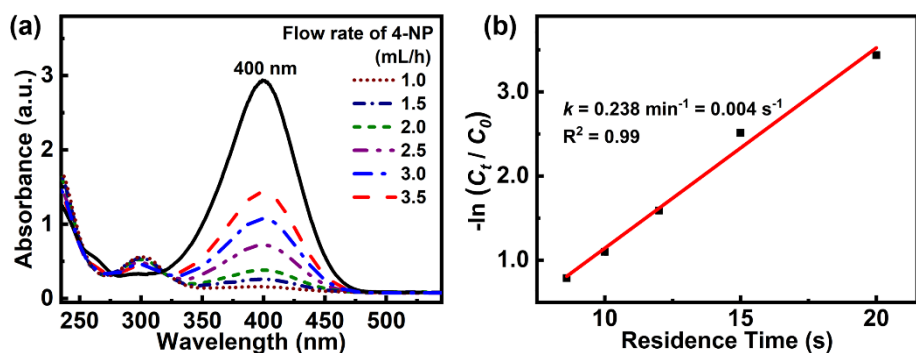


**Fig. S3** (a) UV-Vis spectra for the C-F reduction of 4-NP in the reactor using CoO<sub>x</sub>-coated glass bead as packing material (Solid line represents UV-Vis spectrum of 4-nitrophenolate anions generated by the mixing of NaBH<sub>4</sub> and 4-NP). (b) Plot of  $-\ln(C_t/C_0)$  versus the residence time.

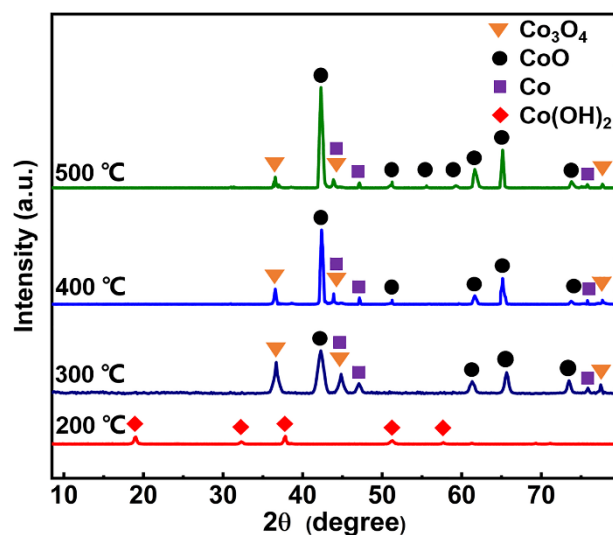


**Fig. S4** XRD patterns of packing materials at different calcination temperatures.

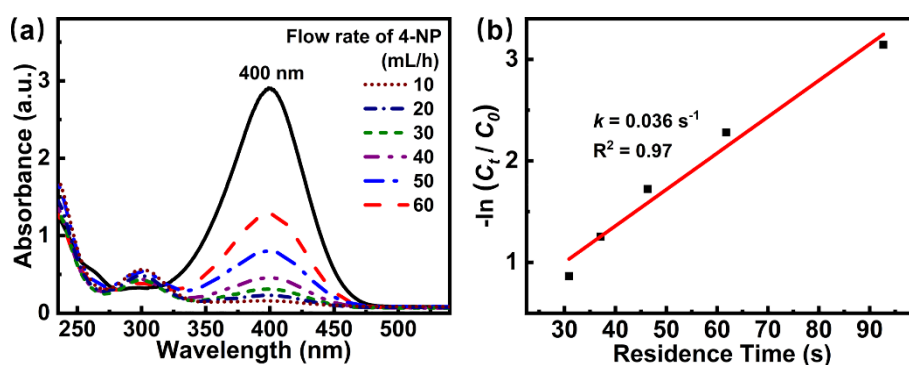


**Fig. S5** (a) UV-Vis spectra for the C-F degradation of 4-NP in the reactor using Au-coated glass bead as packing material (Solid line represents UV-Vis spectrum of 4-nitrophenolate anions generated following the mixing of  $\text{NaBH}_4$  and 4-NP). (b) Plot of  $-\ln(C_t/C_0)$  versus the residence time.

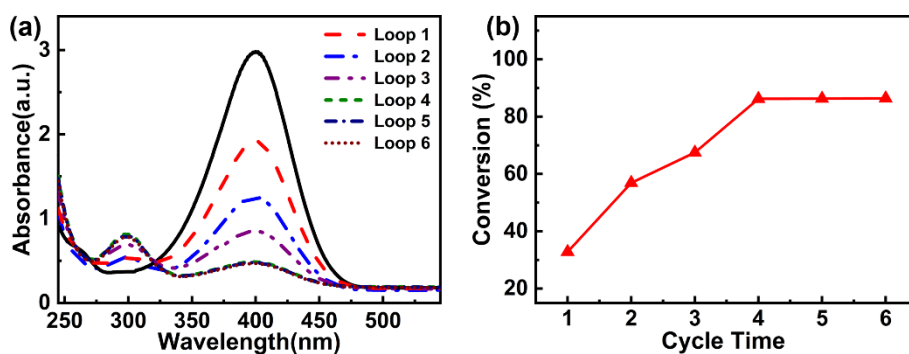


**Fig. S6** (a) UV-Vis spectra for the reduction of 4-NP at different cycles (Solid line represents UV-Vis spectrum of 4-nitrophenolate anions generated by the mixing of  $\text{NaBH}_4$  and 4-NP). (b) The relationship between the conversion efficiency of 4-NP and its cycle time.

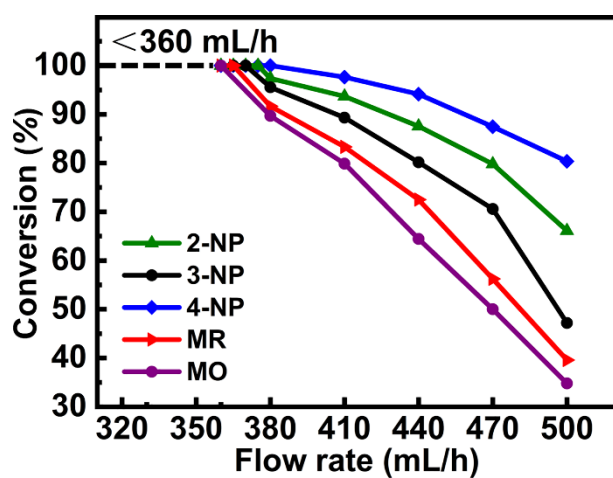


**Fig. S7** Plots of the conversion efficiency of 2-NP, 3-NP, 4-NP, MR and MO versus their flow rates.

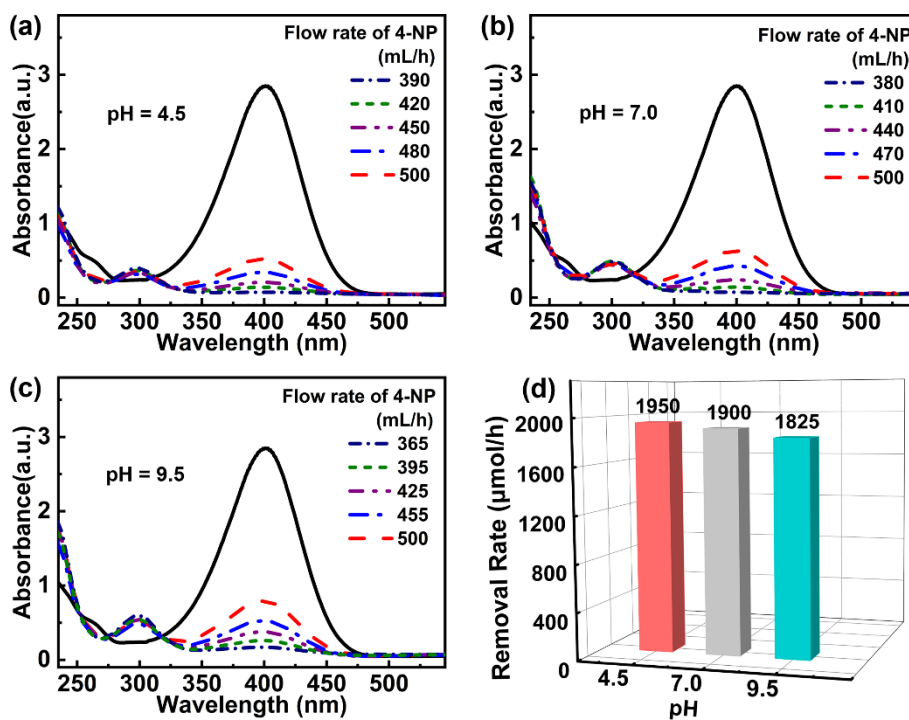


**Fig. S8** (a-c) UV-Vis spectra for the C-F reduction of 4-NP at different pH values of DW (Solid lines represent UV-Vis spectra of 4-nitrophenolate anions generated by following the mixing of  $\text{NaBH}_4$  and 4-NP). (d) The relationship between the removal rate of 4-NP and the pH value.



**Table S5**

Catalytic capacity of catalysts used for the batch reduction of nitro and azo compounds.

Nitro and azo compounds	Catalyst	Concentration (mM)	Conversion (%)	$k \times 10^{-2}$ (s <sup>-1</sup> )	Removal rate (μmol/h)	Ref.
2-NP	Co <sub>3</sub> O <sub>4</sub> @nHAP	0.500	97.8	0.403	25.0	[1]
	Ag@TiO <sub>2</sub>	0.100	97.5	0.031	0.9	[2]
	NiO/AlMCM-41	0.200	100	0.350	2.4	[3].
	Bi <sub>2</sub> O <sub>2</sub> CO <sub>3</sub> /NiFe <sub>2</sub> O <sub>4</sub>	2.000	100	0.350	21.4	[4]
	Tandem Module <sup>a</sup>	5.000	100	36.0	1875 <sup>b</sup>	This work <sup>f</sup>
3-NP	PANI/Au	5.430	100	2.89	194.6	[5]
	SG-AuNPs	1.000	96	0.14	10.7	[6]
	Co-Cu/ZIF	0.150	95	1.85	9.0	[7]
	Tandem Module	5.000	100	34.0	1850 <sup>c</sup>	This work
MO	Au/CeO <sub>2</sub> NPs	0.200	92	0.860	60.0	[8]
	Au-Ag/TiO <sub>2</sub>	0.018	89.4	0.059	10.8	[9]
	AgCl-Cu <sub>2</sub> O	0.012	98.4	0.300	7.2	[10]
	Tandem Module	5.000	100	26.0	1800 <sup>d</sup>	This work
MR	MnFe <sub>2</sub> O <sub>4</sub> @EP@Ag	2.340	99	0.100	0.53	[11]
	ZnFe <sub>2</sub> O <sub>2</sub>	0.002	97	0.044	2.0	[12]
	Tandem Module	5.000	100	28.0	1825 <sup>e</sup>	This work

<sup>a</sup> Au-Co-CoOx-coated glass beads are used as catalyst in the tandem module.<sup>b</sup> Removal rate = Flow rate × Molar concentration × Conversion = 375 mL/h × 5 mM × 100% = 1875 μmol/h<sup>c</sup> Removal rate = Flow rate × Molar concentration × Conversion = 370 mL/h × 5 mM × 100% = 1850 μmol/h<sup>d</sup> Removal rate = Flow rate × Molar concentration × Conversion = 360 mL/h × 5 mM × 100% = 1800 μmol/h<sup>e</sup> Removal rate = Flow rate × Molar concentration × Conversion = 365 mL/h × 5 mM × 100% = 1825 μmol/h<sup>f</sup> In this work, nitro and azo compounds are removed via the C-F reduction.

## References

- [1] D. Serkan, *J. Mol. Struct*, 2021, **1238**, 130390.
- [2] S. M. Albukhari, M. Ismail, K. Akhtar and E. Y. Danish, *Colloids & Surfaces A*, 2019, **577**, 548-561.
- [3] Z. Derikvand, F. Rahmati and A. Azadbakht, *Appl. Organomet. Chem*, 2019, **33**, e4864.
- [4] Z. Parisa and F. Saeed, *J. Alloy. Compd*, 2017, **729**, 1046-1057.
- [5] L. b. Sun, L. Jiang, J. Zhang, T. Murayama, M. Zhang, Y. h. Zheng, H. J. Su and C. X. Qi, *Top. Catal*, 2021, **64**, 215-223.
- [6] V. H. Leab, T.G.Duongc, V. T. Lec, T. L. Phanc, T. L. H. Nguyend, T. P. Chaue and D. V. Doan, *RSC Adv*, 2021, **11**, 15438-15448.
- [7] M. Gholinejad, Z. Naghshbandi and J. M. Sansano, *Appl. Organomet. Chem*, 2020, **34**, 1-10.
- [8] F. Zoulikhaa, A. Nawala, B. F. Taiebb, B. Sumeyaa and B. Redouanea, *J. Environ. Chem. Eng*, 2020, **8**, 104346.
- [9] X. D. Jiang, Z. X. Wang, X. H. Zhang, G. X. Jiang, Y. Peng, S. Xu, M. Cao, X. Dai, Z. H. Liu and J. Y. Ma, *J. Nanopart. Res*, 2019, **21**, 211.
- [10] H. J. Zhao, J. K. Qu, F. Y. Zhou, Z. Q. Zhao, X. Chen, H. W. Xie, Q. S. Song, D. H. Wang and H. Y. Yin, *ACS Sustain. Chem. Eng*, 2021, **9**, 5651-5660.
- [11] G. M. Ulvi, K. Murat, E. Gkhan, Ertrk and A. Serol, *Appl. Organomet. Chem*, 2021, **35**, 1-11.
- [12] T. Tangcharoen, J. T-Thienprasert and C. Kongmark, *Int. J. Appl. Ceram. Tec*, 2021, **18**, 1125-1143.